AGU PUBLICATIONS

JGR

Journal of Geophysical Research: Earth Surface

RESEARCH ARTICLE

10.1002/2016JF003847

Incisional cyclic steps of permanent form in mixed bedrock-alluvial rivers

Norihiro Izumi[1], **Miwa Yokokawa**[2], **and Gary Parker**[3]

[1]Division of Field Engineering for the Environment, Faculty of Engineering, Hokkaido University, Sapporo, Japan, [2]Faculty of Information Science and Technology, Osaka Institute of Technology, Hirakata, Japan, [3]Department of Civil and Environmental Engineering and Department of Geology, University of Illinois at Urbana-Champaign, Urbana-Champaign, Illinois, USA

Key Points:
- The MRSAA incision model is integrated into a hydraulic model to explain the formation of cyclic steps in mixed bedrock-alluvial streams
- The problem is greatly simplified by the quasi-steady approximation: alluvial processes are taken to be much faster than incisional ones
- The analysis explains key features of bedrock cyclic steps: a short adversely sloping upstream portion and a long planar downstream portion

Correspondence to:
N. Izumi,
nizumi@eng.hokudai.ac.jp

Citation:
Izumi, N., M. Yokokawa, and G. Parker (2017), Incisional cyclic steps of permanent form in mixed bedrock-alluvial rivers, *J. Geophys. Res. Earth Surf.*, *122*, 130–152, doi:10.1002/2016JF003847.

Received 7 FEB 2016
Accepted 8 DEC 2016
Accepted article online 17 DEC 2016
Published online 12 JAN 2017

Abstract Most bedrock river channels have a relatively thin, discontinuous cover of alluvium and are thus termed mixed bedrock-alluvial channels. Such channels often show a series of steps formed at relatively regular intervals. This bed form is the bedrock equivalent of cyclic steps formed on beds composed of cohesive soil in gullies. In this paper, we perform a full nonlinear analysis for the case of cyclic steps in mixed bedrock-alluvial channels to explain the formation of these steps. We employ the shallow water equations in conjunction with equations describing the process of bedrock incision. As a model of bedrock incision, we employ the recently introduced Macro-Roughness Saltation Abrasion Alluviation model, which allows direct interaction between alluvial and bedrock morphodynamics. The analysis is greatly simplified by making the quasi-steady assumption that alluvial processes occur much faster than bedrock erosional processes. From our analysis, we obtain the conditions for the formation of cyclic steps in bedrock, as well as the longitudinal profiles of bed elevation, water surface elevation, and areal fraction of alluvial cover. It is found from the analysis that when the sediment supply is small relative to the transport capacity, cyclic steps form only on slopes with very high gradients. The analysis indicates that the shape of a step formed on bedrock is characterized by a relatively short upstream portion with an adverse slope and a long, almost planar downstream portion with a constant slope.

1. Introduction

Where sediment transport capacity is dominant over sediment supply, as is commonly the case in mountain river reaches, it is often observed that bedrock is locally exposed in parts of the riverbed. If the riverbed is completely alluviated, even if the cover is thin, the channel may be able to reach a dynamic equilibrium associated with a constant sediment supply rate, without any bed degradation. A change in conditions (e.g., flow acceleration) is required to initiate bed degradation and eventually expose bedrock. If, however, the supply rate is insufficient to keep the bed covered with alluvium when the river is morphologically active, the bedrock can be very slowly, but repeatedly, eroded during floods, so that the cumulative bed incision over time can be substantial.

In recent years in particular, bedrock has been increasingly exposed in rivers throughout Japan, even in moderate-gradient reaches [*Yamamoto*, 2010]. This might be due to the decrease in sediment supply from mountain regions associated with dam construction and excessive erosion control. Bedrock exposure and erosion and the resulting bed degradation have caused the destabilization of river structures such as bridge piers and bank revetments [*Yonezawa et al.*, 2007; *Tadatsu et al.*, 2009; *Mori et al.*, 2010; *Inoue et al.*, 2011]. In addition, bedrock rivers that are devoid of sediment can provide very poor habitat for aquatic animals, as compared to mixed bedrock-alluvial or purely alluvial rivers [*Inoue et al.*, 2011]. Therefore, the problem of bedrock exposure is important from an environmental as well as engineering point of view.

In such rivers with exposed bedrock, a series of steps is commonly observed to form at relatively uniform intervals. These steps are bedrock equivalents to cyclic steps formed on beds composed of cohesive soil [*Parker and Izumi*, 2000]. *Kostic et al.* [2010] provide an overview of cyclic steps in diverse settings, including those formed by flowing water in different stream types (alluvial, bedrock, and cohesive sediment) and by turbidity currents on the seafloor. Cyclic steps can also form on ice, for example, due to katabatic winds on Mars [*Smith et al.*, 2013] or flowing water in supraglacial streams (Figure 1a), a process that has recently been

Figure 1. Cyclic steps observed in a variety of environments. (a) Cyclic steps in a supraglacial meltwater stream on the Llewellyn Glacier, British Columbia, Canada. An ice ax on the right bank with a length of about 0.7 m provides scale. Photo courtesy of Leif Karlstrom; more information about the site is provided in *Karlstrom et al.* [2014]. (b) Cyclic steps in the Nanatsugama Reach in Nishizawa Canyon, Yamanashi, Japan. The reach displays five successive steps, four of which are shown in the image. Step height is 2–3 m. Both exposed bedrock and alluvium can be seen just upstream of the lip of the step farthest downstream in the image. Image courtesy Yamanashi City Tourist Association. (c and d) Two steps of a train of cyclic steps in cohesive material in a discontinuous gully on the Loess Plateau, China. The step in Figure 1d is immediately downstream of the step in Figure 1c. There were over 11 steps in the gully at the time of the photograph (2012). The spacing between steps was of the order of tens of meters. The bed consists of weakly cohesive silty loess with no obvious internal structure, and no sand or gravel, and with a grass cover that is too sparse to protect against the entrainment of dust by even a mild wind.

studied in a laboratory flume [*Yokokawa et al.*, 2016]. Although in principle the terminology could apply to any streamwise train of steps in a channel, here we mean steps that are self-formed by a morphodynamic interaction between the bed and the flow above it. In addition, the flow over these steps under formative conditions is Froude-transcritical; each step contains an upstream region of subcritical flow followed by a downstream region of supercritical flow and is bounded upstream and downstream by hydraulic jumps [*Parker and Izumi*, 2000; *Kostic et al.*, 2010] (see also Figure 2). Finally, the train of steps tends to migrate upstream. Here we study the case of cyclic steps, as defined above, in mixed bedrock-alluvial rivers. It should be noted that there are indeed periodic trains of steps in bedrock rivers, driven allogenically by faults or variation in erodibility [*Goode and Wohl*, 2010a, 2010b], but these are not the subject of our analysis.

Examples of cyclic steps have been observed extensively in mixed bedrock-alluvial rivers [*Duckson and Duckson*, 1995]. One such example, the five steps of Nanatsugama in Nishizawa Canyon, Yamanashi, Japan, is illustrated in Figure 1b. Both exposed bedrock and alluvium can be seen just upstream of the lip of the step

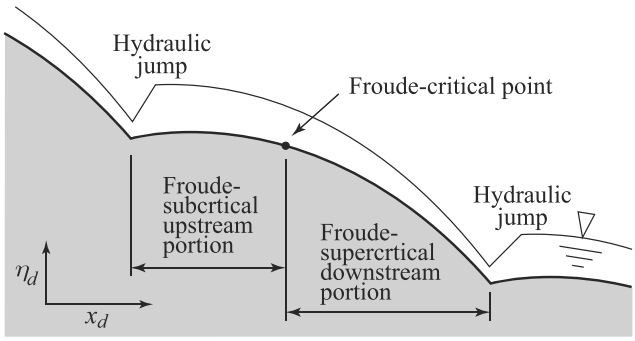

Figure 2. Conceptual diagram of cyclic steps.

farthest downstream. Although real-time documentation of the evolution of these steps is not available to us, direct inspection by one of us (Yokokawa) shows that (a) gravel deposited on the downstream lip of the plunge pool armors the bedrock and is covered by moss, suggesting that the clasts have not moved recently, whereas gravel deposited at the upstream end of the plunge pool shows evidence of having moved vigorously and collided with the bed during plunging flow, suggesting the potential for upstream migration of these steps, and (b) the apparent absence of externally imposed constraints (such as faults) suggests that these steps are indeed autogenic. Direct observation for formation of autogenic cyclic steps associated with hydraulic jumps can be seen in the experimental bedrock-alluvial steps of *Yokokawa et al.* [2013], *Scheingross et al.* [2015], and *Scheingross* [2016, chap. 6 therein]; upstream migration is also described in the latter two references. Here we pursue a physically based analysis to explain these steps. More specifically, we assume that the mechanism for differential incision of the steps into bedrock is abrasion caused by alluvial particles colliding with the bedrock surface and that the spatial pattern of incision is governed by an interaction between alluvial transport over a partially covered bedrock surface and the fluid mechanics of Froude-transcritical flow.

The first analytical study on cyclic steps was performed by *Parker and Izumi* [2000]. They considered the case of incisional steps in a cohesive bed which could be eroded by the force of the flow alone, without the aid of tools such as stones to cause wear. The cyclic steps that form in such a setting have also been termed "discontinuous gullies" [*Reid*, 1989]. Figures 1c and 1d illustrate the form of these steps in a gully on the Loess Plateau of China. The bed consists of poorly consolidated silt with an absence of internal structure. This material is easily eroded by the direct action of flow alone. The channel bed consists of sparse grass growing directly from the loess, with no layer of loose sediment. *Parker and Izumi* [2000] showed that the interaction of Froude-transcritical flow over a bed eroded by the direct action of water allows the formation of upstream-migrating trains of steps. The analytical framework admits a solution of permanent form, in which the train of steps incises and migrates upstream both at constant rates but otherwise does not change in morphology. The analysis we consider here falls within the same framework as *Parker and Izumi* [2000], but the way in which incision is treated is fundamentally different. The importance of tools for incision in the case of steps in mixed bedrock-alluvial streams, and their lack of relevance in the case of gullies in cohesive material, can be appreciated by comparing Figures 1b–1d.

Since the work of *Parker and Izumi* [2000], a number of studies have been devoted to the analytical and numerical modeling of cyclic steps in a variety of environments. For example, *Sun and Parker* [2005] found solutions of permanent form for cyclic steps in alluvium. *Kostic and Parker* [2006] and *Fildani et al.* [2006] have numerically modeled cyclic steps created by turbidity currents. *Yokokawa et al.* [2016] provide an analytical framework which describes incipient (but not fully formed) cyclic steps at ice-water interfaces.

The key to the analysis of cyclic steps in the case of bedrock-alluvial channels is in the treatment of alluvial-bedrock interaction. Here we use a modified version of the saltation-abrasion model of bedrock wear due to colliding bed load particles first proposed by *Sklar and Dietrich* [2004]. We embed this model into the Macro-Roughness Saltation Abrasion Alluviation (MRSAA) model of bedrock-alluvial morphodynamics of *Zhang et al.* [2015].

2. Formulation

2.1. Erosion of Bedrock

In bedrock rivers, one way that bedrock can be eroded is by the process of abrasion due to gravel bed load particles striking exposed bedrock. Formulations of this abrasion process have been proposed by several researchers. Among them, *Sklar and Dietrich* [2004] described the erosion rate E_d (length/time) in the form

$$E_d = \beta q_{ad}\left(1 - \frac{q_{ad}}{q_{acd}}\right) \tag{1}$$

where β is an abrasion coefficient with the dimension of (length scale)$^{-1}$ and q_{ad} is the volumetric gravel transport rate per unit width. In addition, q_{acd} is the volumetric gravel transport capacity per unit width that would prevail were the bed completely alluviated with no exposed bedrock, a parameter which we assume to be determined solely by the local bed shear stress. In the above equation, then, the term $1 - q_{ad}/q_{acd}$ reflects the fact that some fraction of bed surface area may be composed of exposed bedrock rather than alluvium. The bedrock erosion function defined above, including both effects of sediment availability and partial alluvial cover is a landmark contribution to the morphodynamics of bedrock rivers. However, there is a limitation on the application of the model of *Sklar and Dietrich* [2004], in the sense that q_{ad} represents the sediment transport rate limited by the sediment supply which is not directly connected to local morphodynamics [*Zhang et al.*, 2015].

Any global tendency toward riverbed incision is likely determined by conditions of sediment supply from upstream. However, when we focus on a local river reach, the net sediment discharge should be strongly affected by local hydraulic parameters and bed topography of the surrounding area. Based on this idea, *Izumi and Yokokawa* [2011], *Izumi et al.* [2012], and *Tanaka and Izumi* [2013] have made a modification of Sklar and Dietrich's model [*Sklar and Dietrich*, 2004]. They assume that the cover fraction p, defined as the local mean areal fraction of bedrock surface covered with alluvium, is determined by the balance between the rates at which sediment enters and leaves the site in question. They employ a form of the Exner equation of sediment continuity adapted to include partial cover to describe the spatial variation of p. Recently, *Zhang et al.* [2015] have introduced the concept of a macroroughness intrinsic to bedrock into this modified formulation. Their model, which is termed the Macro-Roughness Saltation Abrasion Alluviation (MRSAA) model, is explained in detail below.

In the MRSAA model, bedrock is assumed to have a geometric roughness with the characteristic length scale L_{mrd}, here called a macroroughness (so as to distinguish it from the roughness height that enters into the logarithmic velocity law for turbulent flow over a hydraulically rough bed). Where the local sediment supply is small relative to the transport capacity, any deposition that occurs will be discontinuous, causing infilling of local interstices, but not completely covering the bedrock, which remains widely exposed. As the local sediment transport rate increases, the exposed area of bedrock decreases, and when the local sediment supply increases above some value corresponding to a capacity state, the bedrock is fully covered with sediment.

The elevation of the bedrock at the base of the macroroughness elements is denoted by η_{bd}. The time variation of η_{bd} corresponds to the incision rate $-E_d$, where E_d can be described by (1) rewritten by the use of the cover fraction p representing the areal fraction of the bed that is covered with alluvium [*Zhang et al.*, 2015]. That is,

$$\frac{\partial \eta_{bd}}{\partial t_d} = -\beta p q_{acd}(1-p) \tag{2}$$

where t_d is time. In these variables, the subscript d indicates a dimensional variable that will later be represented in dimensionless form with the subscript removed.

Denoting the local mean thickness of alluvium deposited on bedrock by η_{ad}, the time variation of η_{ad} can be assumed to be expressed by the sediment continuity equation of the form

$$p\frac{\partial \eta_{ad}}{\partial t_d} = -\frac{1}{1-\lambda}\frac{\partial p q_{acd}}{\partial x_d} \tag{3}$$

where λ is the porosity of the alluvium and x_d is the streamwise coordinate. The cover fraction p on the left in the above equation expresses the fact that the time variation of η_{ad} takes place only in part of the bed

covered with alluvium. As described above, the cover fraction p can be expected to increase with the alluvium thickness η_{ad}. The simplest quantification that captures this tendency is as follows:

$$p = \begin{cases} \frac{\eta_{ad}}{L_{mrd}} & \text{when } 0 \le \eta_{ad} \le L_{mrd} \\ 1 & \text{when } \eta_{ad} > L_{mrd} \end{cases} \tag{4}$$

Here L_{mrd} is the macroroughness height. The implication of the above equation is that when the alluvial thickness is smaller than the macroroughness height, the local areal fraction of the bed that is covered with sediment rather than exposed bedrock, i.e., the areal cover fraction p, is equal to the ratio of the alluvial thickness to the macroroughness height, and p is unity when the alluvial thickness is larger than the macroroughness height (thus completely burying the roughness elements). The total bed elevation η_d is then expressed by

$$\eta_d = \eta_{ad} + \eta_{bd} \tag{5}$$

2.2. Flow Equations

As noted above, cyclic steps are a series of upstream-migrating steps, each of which is composed of a gently (or adversely) sloping Froude-subcritical upstream portion, and a steeply sloping Froude-supercritical downstream portion as shown in Figure 2. Though the downstream transition from the mild to steep bed slope is continuous, the transition from the steep to mild bed slope is discontinuous. Correspondingly, subcritical flow on the mild slope gradually accelerates to supercritical flow as slope increases downstream, whereas the transition from supercritical flow on the steep slope to subcritical flow on the mild slope is abrupt and is accompanied by a hydraulic jump. In this paper, the upstream end of a step is defined as the location just downstream of a hydraulic jump, and the downstream end is defined as the location just upstream of the next hydraulic jump.

When the characteristic length scale of change in the streamwise direction is much larger than that in the upward normal (approximately vertical) direction, the flow can be described by the shallow water equations of momentum and mass balance:

$$u_d \frac{\partial u_d}{\partial x_d} = -g\frac{\partial h_d}{\partial x_d} - g\frac{\partial \eta_d}{\partial x_d} - \frac{\tau_{bd}}{\rho h_d} \tag{6}$$

$$u_d h_d = q_{wd} \tag{7}$$

where u_d, h_d, η_d and x_d are the depth-averaged velocity, flow depth, total bed elevation, and horizontal streamwise coordinate, respectively, g is the gravitational acceleration (= 9.8 m/s^2), ρ is the water density (= 1000 kg/m^3), and q_{wd} is the flow discharge per unit width, here assumed to be constant. Note that here we have applied the standard quasi-steady assumption of alluvial morphodynamics, according to which the characteristic time for morphological change of the bed (such as the formation of cyclic steps) is very slow compared to the characteristic time for the flow to respond to changed bed, thus allowing us to drop the time derivative terms in the above equations. In (6), τ_{bd} is the bed shear stress, which we relate to the bed friction coefficient C_f in the form

$$\tau_{bd} = \rho C_f u_d^2 \tag{8}$$

The bed friction coefficient C_f is in general a weak function of relative flow depth (flow depth/roughness height), but here we assume it to be a constant for simplicity. This issue is discussed in more detail below.

The volumetric sediment transport rate per unit width over a completely alluviated bed is here denoted as q_{acd}, where the subscript c denotes capacity. At this point it is not necessary to specify a relation for this sediment transport rate. It is enough to assume that the transport rate increases monotonically with bed shear stress τ_{bd}, and thus in accordance with (8), flow velocity u_d.

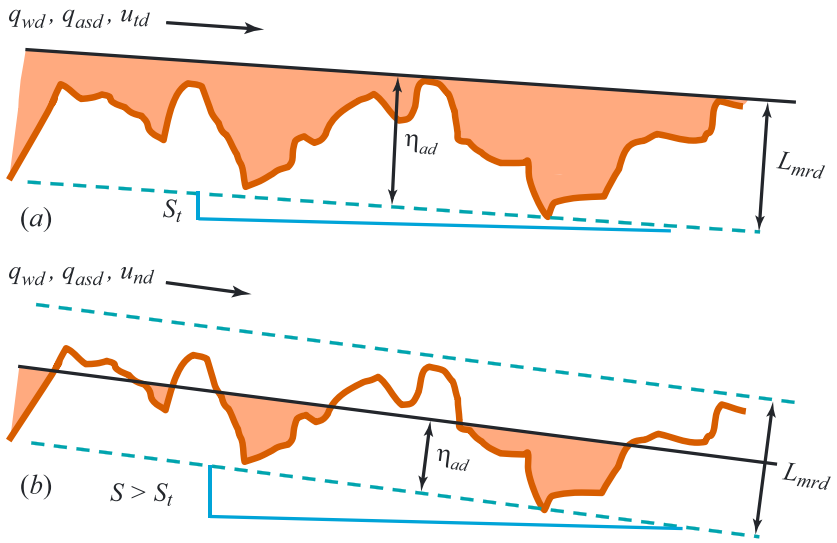

Figure 3. Definition diagram for (a) normal threshold state with bed slope S_t at which the bed is barely alluviated and (b) normal equilibrium state with $S > S_t$, so that the bedrock is only partially covered with alluvium. All other parameters remain the same for Figures 3a and 3b.

3. Theoretical Development

3.1. Threshold State for Incision

As illustrated in Figure 3a, a steady, uniform (normal) threshold state for incision prevails when the bedrock is just barely drowned in alluvium, so that $p = 1$ and according to (2), $\partial\eta_{bd}/\partial t_d = 0$. Once water discharge q_{wd}, alluvial sediment supply rate q_{asd}, and a sediment discharge relation are specified, the threshold slope S_t at which this supply rate corresponds to the capacity rate can be computed. In this steady, uniform threshold state for incision, (6) reduces with (7) and (8) to

$$C_f Fr_t^2 = S_t, \tag{9a}$$

$$Fr_t^2 = \frac{u_{td}^3}{g q_{wd}} \tag{9b}$$

where u_{td} denotes the flow velocity at this threshold state. The corresponding depth h_{td} at the threshold state is then given as q_{wd}/u_{td}.

As assumed implicitly at the beginning of section 1, and in the above paragraph, we assume that the sediment supply rate q_{asd} is constant at least during floods when significant bedrock incision takes place. However, it is recognized that sediment supply in steep mountain rivers can be episodic, exhibiting both short-term variation and long-term variation [*Ashida et al.*, 1981; *Benda and T. Dunne*, 1997a, 1997b; *Montgomery and Buffington*, 1997; *Istanbulluoglu et al.*, 2004]. As such, our assumption of constant sediment supply is not strictly valid. Nevertheless, for our purposes the issue is the relative difference in time scale between the variation of sediment supply and the bed evolution due to bedrock incision. If the time scale of bed evolution is much longer than that of the variation of sediment supply, the assumption of constant sediment supply is expected to be a good approximation. This notwithstanding, even if the time scale of the bed evolution is equivalent to or shorter than that of the variation of sediment supply, the assumption of constant sediment supply corresponds to the first and simplest approximation to employ in studying a problem with more complex elements, i.e., the process of formation of incisional cyclic steps on bedrock.

3.2. Nondimensionalization and Quasi-Steady Assumption of Alluvial Processes

We use the above-defined threshold state to render the governing equations dimensionless. As noted above, no incision can occur at the threshold state, because $p = 1$. This notwithstanding, the parameter βq_{asd}, the alluvial sediment supply rate multiplied by the abrasion coefficient, can serve as a scale for the incision rate, in so far as p is a nondimensional variable between 0 and 1 in (2). The time for the bed to erode one depth h_{td}

thus scales as $h_{td}/(\beta q_{asd})$. We use the backwater length h_{td}/S_t as a horizontal length scale. We then employ the following equations to nondimensionalize the problem:

$$t = \frac{t_d}{h_{td}/(\beta q_{asd})}, \tag{10a}$$

$$x = \frac{x_d}{h_{td}/S_t}, \tag{10b}$$

$$q_{ac} = \frac{q_{acd}}{q_{asd}}, \tag{10c}$$

$$\left(\eta, \eta_a, \eta_b, L_{mr}\right) = \left(\eta_d, \eta_{ad}, \eta_{bd}, L_{mrd}\right)/h_{td} \tag{10d}$$

Here the parameters $t, x, q_{ac}, \eta, \eta_a, \eta_b$, and L_{mr} are the dimensionless versions of their dimensioned corresponding counterparts t_d, x_d, q_{acd}, η_d, η_{ad}, η_{bd}, and L_{mrd}. With the use of the above nondimensionalization, (2)–(5) can be rewritten in the forms

$$\frac{\partial \eta_b}{\partial t} = -pq_{ac}(1-p) \tag{11}$$

$$\gamma p \frac{\partial \eta_a}{\partial t} = -\frac{\partial pq_{ac}}{\partial x} \tag{12}$$

$$p = \begin{cases} \frac{\eta_a}{L_{mr}} & \text{when } 0 \le \eta_a \le L_{mr} \\ 1 & \text{when } \eta_a > L_{mr} \end{cases} \tag{13}$$

$$\eta = \eta_a + \eta_b \tag{14}$$

where the nondimensional parameter γ is

$$\gamma = \frac{\beta q_{asd}}{q_{asd}/[(1-\lambda)h_{td}/S_t]} = \frac{(1-\lambda)\beta h_{td}}{S_t} \tag{15}$$

The numerator and the denominator of γ scale the characteristic erosion rate of bedrock, and the typical speed of alluvial sediment deposition and erosion, respectively; therefore, γ represents the ratio between the two (referred to as the incisional-alluvial speed ratio, hereafter). Here we consider the common case of bedrock that is so strong that the bedrock erosion is much slower than alluvial processes, so that γ is expected to be small. (This condition is not universal: in some cases the bedrock is so weak and erosion prone that it is alluvial cover that prevents rapid degradation [*Tanise et al.*, 2008].) Thus, assuming $\gamma = 0$ and dropping the terms with γ in (12) is equivalent to ignoring the unsteadiness of the alluvial process. This corresponds to a second quasi-steady condition in addition to the standard quasi-steady assumption for the flow introduced above, according to which flow can be assumed to be steady in morphodynamic problems. According to this second condition, alluvial thickness η_{ad} is assumed to respond quickly to changes in bedrock elevation η_{bd}. Under this constraint, at the time scale of bedrock erosion, the alluvial thickness η_{ad} responds "immediately," so that alluvial processes can be assumed to be steady. In this paper, the assumption that alluvial processes can be assumed to be steady is referred to as the "quasi-steady assumption of alluvial processes."

Dropping terms multiplied by γ with the use of the quasi-steady assumption of alluvial processes in (12), we obtain the result that the nondimensional net volumetric gravel transport rate q_a equivalent to pq_{ac} must be constant in space. Because this constant volumetric gravel transport rate is nothing other than the dimensionless alluvial sediment supply rate q_{as}, which is equivalent to unity as all the quantities of sediment transport rate are nondimensionalized by the dimensional alluvial sediment supply rate q_{asd}, we obtain

$$pq_{ac} = 1 \tag{16}$$

The above equation implies that the areal cover fraction p is inversely proportional to the dimensionless volumetric gravel transport capacity q_{ac}. In so far as it is assumed that the sediment supply is constant, and the volumetric gravel transport rate increases with increasing bed shear stress, it follows that the cover fraction p decreases with increasing bed shear stress and increases with decreasing bed shear stress. In other words,

under the condition that the sediment transport rate is constant but below capacity ($q_{acd} > q_{asd}$, or $q_{ac} > 1$ in the dimensionless form), a relatively large alluvial cover fraction (p close to the maximum value of unity) prevails in reaches where the dimensionless sediment transport capacity is small (q_{acd} is close to the minimum value q_{asd}, or q_{ac} is close to the minimum value of unity in the dimensionless form), whereas a relatively small cover fraction ($p \ll 1$) prevails in reaches where the dimensionless sediment transport capacity is large ($q_{acd} \gg q_{asd}$, or $q_{ac} \gg 1$ in the dimensionless form).

From (13) and (16), the alluvial thickness η_a is expressed in the form

$$\eta_a = \frac{L_{mr}}{q_{ac}} \tag{17}$$

With the use of (16), (11) reduces to

$$\frac{\partial \eta_b}{\partial t} = -\left(1 - q_{ac}^{-1}\right) \tag{18}$$

From (14), (17), and (18), we find that the time variation of the total bed elevation η is expressed by the relation

$$\frac{\partial \eta}{\partial t} = L_{mr}\frac{\partial q_{ac}^{-1}}{\partial t} - \left(1 - q_{ac}^{-1}\right) \tag{19}$$

3.3. Conditions at the Upstream End of a Step

Parker and Izumi [2000] employed the assumption that a threshold condition is achieved at the upstream end of a step in the analysis of cyclic steps by flow over a cohesive bed. This is because, even though solutions for cyclic steps are possible without this assumption, such solutions may represent unstable finite amplitude equilibria. That is, any small perturbation would result in the initiation of erosion at the upstream end of each step, which would then only be completely stabilized when the threshold condition for bed erosion is achieved just beyond the hydraulic jump. The same assumption is made in this treatment of bedrock incision as well. (This is only a local condition; it is shown below that the train of steps as a whole can continue to incise downstream, because the point of zero incision corresponds to an upstream moving boundary.) According to (2), bedrock incision vanishes either when the net volumetric gravel transport rate vanishes ($pq_{acd} = 0$), or when the bedrock is fully covered with sediment ($p = 1$). Because pq_{acd} is constant in space, if pq_{acd} were to vanish at the upstream end, there would be no sediment transport anywhere on the step, thus resulting in no bed erosion anywhere either. In so far as we are not interested in this case, we assume that at the upstream end of the reach (just downstream of a hydraulic jump), the bedrock is fully but barely covered with sediment, and thus $p = 1$ there. In addition, the condition $p = 1$ must be achieved only precisely at the upstream end because, if there were a finite reach where no erosion takes place, cyclic steps of permanent form migrating upstream with constant wave velocity (see Figure 5 subsequently shown) could not exist. (Indeed, were a train of steps subject to erosion without downcutting, not only could a permanent form not be maintained, but the steps themselves would be completely obliterated.) As a result, the following incision threshold condition (not to be confused with the threshold of motion of the gravel) is satisfied right at the upstream end of a step:

$$q_{ac} = 1 \tag{20}$$

Since the upstream end of a step is immediately downstream of a hydraulic jump, it follows that the Froude number at this point of incision threshold should be less than unity, i.e., $Fr = Fr_t < 1$.

3.4. Equilibrium Incision in the Absence of Steps

In addition to the threshold state for incision, it is of value to define one more steady, uniform (normal) state, i.e., that corresponding to incision in the absence of steps. Nondimensional parameters defined in these two steady uniform states are helpful for facilitating the subsequent analysis. Variables in this normal state are denoted by the subscript n, which denotes "normal." To define this uniform state, we consider a flow for which all parameters (including water discharge per unit width q_{wd} and sediment supply rate q_{asd}) are the same as the threshold state except the bed slope S, which is now taken to be higher than S_t. As shown in Figure 3b, this perforce corresponds to a cover fraction at this normal state satisfying the condition $p_n < 1$, so that the bed

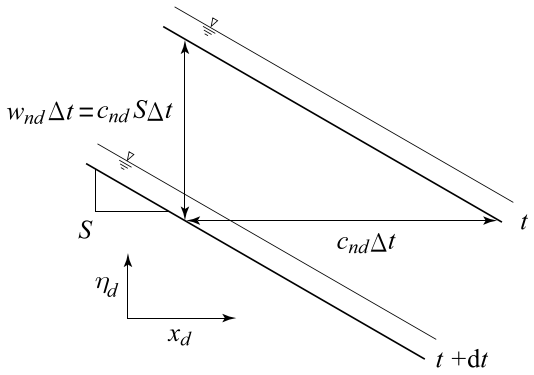

Figure 4. Conceptual diagram for bed erosion in the absence of steps.

incises everywhere. The normal flow velocity at this state u_n accordingly exceeds u_t. Denoting Froude number corresponding to this equilibrium state by Fr_n, we obtain the relations

$$C_f Fr_n^2 = S, \tag{21a}$$

$$Fr_n^2 = \frac{u_{nd}^3}{g q_{wd}} \tag{21b}$$

Note that since $S > S_t$, it follows that $Fr_n > Fr_t$. Since the bed is only partially covered with sediment, it undergoes incision at the dimensionless vertical rate w_n and corresponding dimensioned rate w_{nd}, where

$$w_n = \frac{w_{nd}}{\beta q_{asd}} = p_n q_{acn}(1 - p_n) = 1 - \frac{1}{q_{acn}} \tag{22}$$

In the above equation, q_{acn} denotes the nondimensional capacity sediment transport rate at the equilibrium (normal-flow) incision condition in the absence of steps. The condition that the sediment transport rate be equal to the supply yields the dimensioned relation $q_{asd} = p_n q_{acnd}$ where q_{acnd} is the dimensioned version of q_{acn}, or rewriting in dimensionless form with (10c), $1 = p_n q_{acn}$.

As shown in Figure 4, there is a simple geometrical relation $w_{nd} = c_{nd} S$ between the constant (dimensioned) vertical bed degradation rate w_{nd} and the constant (dimensioned) rate of upstream migration of the bed profile in the absence of steps c_{nd}. Nondimensionalizing c_{nd} by $\beta q_{asd}/S_t$, we obtain the following relation between w_n and c_n:

$$w_n = c_n S_r, \tag{23a}$$

$$S_r = \frac{S}{S_t} \tag{23b}$$

In addition, from (9a) and (9b), and (21a) and (21b), S_r can be expressed in terms of Fr_t and Fr_n by the relation

$$S_r = \frac{Fr_n^2}{Fr_t^2} \tag{24}$$

3.5. Cyclic Steps of Permanent Form

Certain systems of equations admit solutions of permanent form. That is, after translation to account for constant migration rates in the streamwise and vertical direction, the governing equations reduce to a form in which only spatial variation remains. A classical case of a solution of permanent form is that for roll waves: there is a state at which the waves are periodic in space and migrate upstream at a constant speed [e.g., *Balmforth and Vakil*, 2012]. *Parker and Izumi* [2000] have shown that the equations governing cyclic steps in cohesive material admit a solution of permanent form. Here we demonstrate that a similar solution exists for the case of cyclic steps in mixed bedrock-alluvial streams. That is, the wave train of steps migrates upstream and downward at constant rates, but otherwise does not change in time. In order to describe a stepped bed migrating

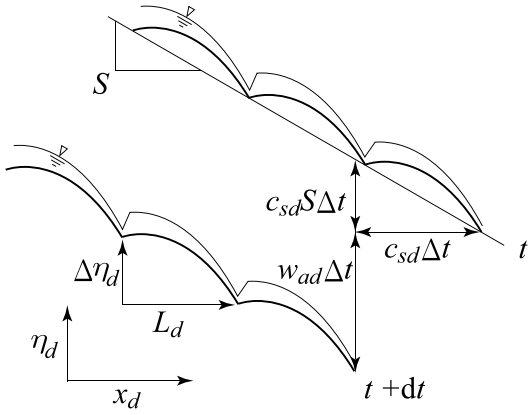

Figure 5. Conceptual diagram for bed erosion in the presence of steps.

upstream with nondimensional wave speed c, and a nondimensional additive degradation rate additional to that caused by a parallel shift in the horizontal direction w_a, we introduce the expression for η in the form

$$\eta(x,t) = \tilde{\eta}(\tilde{x}) - w_a t, \tag{25a}$$

$$\tilde{x} = x + ct \tag{25b}$$

where the tilde indicates a coordinate moving with steps and c and w_a are parameters that have been made dimensionless from their corresponding dimensional parameters c_d and w_{ad} using the scales $\beta q_{asd}/S_t$ and βq_{asd}, respectively. In general, the upstream migration rate in the presence of steps c is different from the value c_n in the absence of steps. In addition, w_a is not a total vertical degradation rate, but instead a vertical degradation rate additional to that associated with degradation caused by purely horizontal migration (see Figure 5). Denoting the wavelength nondimensionalized by h_{td}/S_t by L, and the wave height nondimensionalized by h_{td} by $\Delta\eta$, we obtain the following relation:

$$\Delta\eta = \tilde{\eta}(\tilde{x}) - \tilde{\eta}(\tilde{x} + L) \tag{26}$$

In this paper, we idealize the problem to an infinitely long river channel with a constant mean bed slope, so that upstream and downstream influences never extend into the target domain. When this assumption is applied to the case of bedrock erosion considered in this paper, the mean bed slope is a prescribed value equal to the bed slope S in the absence of steps, as shown in Figure 4. Keeping in mind the vertical and horizontal length scales used in the nondimensionalization, the slope S can be written, with the use of $\Delta\eta$ and L, in the form

$$\frac{S}{S_t} = S_r = \frac{\Delta\eta}{L} \tag{27}$$

The total nondimensional vertical degradation rate w_s is then

$$w_s = -\overline{\frac{\partial\eta}{\partial t}} \tag{28}$$

where the overbar denotes averaging over one wavelength, defined as $\overline{F} = \int_{\tilde{x}}^{\tilde{x}+L} F(\xi)\,\mathrm{d}\xi/L$. Substituting (25a) and (25b) into (28), we obtain

$$w_s = w_a - c\overline{\frac{\mathrm{d}\tilde{\eta}}{\mathrm{d}\tilde{x}}} = w_a + cS_r \tag{29}$$

It is found from the above equation that the total vertical degradation rate w_s is the sum of the vertical degradation caused by horizontal migration cS_r and the additional vertical degradation rate w_a as shown in Figure 5.

Nondimensionalizing the velocity and flow depth in (6) and (7) by u_{td} and h_{td} respectively, substituting with (25a) and (25b), and eliminating h, we obtain

$$\left(Fr_t^2 u - u^{-2}\right)\frac{\mathrm{d}u}{\mathrm{d}x} = -\frac{\mathrm{d}\eta}{\mathrm{d}x} - u^3 \tag{30}$$

where the ~ has been (and is henceforth) dropped for simplicity. Substituting (25a) and (25b) into (19), and dropping ~ again, we obtain

$$c\frac{\mathrm{d}\eta}{\mathrm{d}x} = w_a + cL_{mr}\frac{\mathrm{d}q_{ac}^{-1}}{\mathrm{d}x} - \left(1 - q_{ac}^{-1}\right) \tag{31}$$

Substitution of the above equation into (30) yields

$$\frac{\mathrm{d}u}{\mathrm{d}x} = \frac{c^{-1}\left(1 - q_{ac}^{-1} - w_a\right) - u^3}{Fr_t^2 u - u^{-2} - L_{mr} q_{ac,u} q_{ac}^{-2}} \tag{32}$$

where $q_{ac,u} = \partial q_{ac}/\partial u$. The spatial distribution of velocity u can be obtained by integrating the above equation with respect to x.

Taking the origin of x at the upstream end of a step, where the threshold condition for bed incision (barely complete alluvial cover) is achieved, we have the following boundary condition:

$$u(0) = 1 \tag{33}$$

At the downstream end of a step, the flow condition just before the next hydraulic jump downstream is realized. The flow velocity must thus be equal to the conjugate value of the velocity at $x = 0$. That is,

$$u(L) = \left[\frac{\left(1 + 8Fr_t^2\right)^{1/2} - 1}{2}\right]^{-1} \tag{34}$$

Once u is obtained as a function of x, (31) can be integrated with respect to x, and the distribution of η can be obtained in the form

$$\eta(x) = L_{mr}\left[q_{ac}^{-1}\left(u(x)\right) - q_{ac}^{-1}(u_L)\right] + \frac{(1 - w_a)(L - x)}{c} - \frac{1}{c}\int_x^L q_{ac}^{-1}\left(u(\xi)\right)\mathrm{d}\xi \tag{35}$$

where $u_L = u(L)$. Substituting $x = 0$ in the above equation, we obtain the following relation for step height $\Delta\eta$:

$$\Delta\eta = L_{mr}\left[1 - q_{ac}^{-1}(u_L)\right] + \frac{(1 - w_a)L}{c} - \frac{L}{c}\overline{q_{ac}^{-1}} \tag{36}$$

Modifying the above equation with the use of (24), (26), and (27), we obtain

$$w_a = 1 - \overline{q_{ac}^{-1}} + c\left[\frac{L_{mr}}{L}\left(1 - q_{ac}^{-1}\right) - \frac{Fr_n^2}{Fr_t^2}\right] \tag{37}$$

This equation specifies the relation between w_a, c, L, Fr_n, and Fr_t.

3.6. Bed Load Function

In order to integrate (32), the capacity transport rate q_{ac} has to be specified as a function of velocity u. Here we assume that the mode of sediment transport is bed load. In addition, we assume for simplicity that the sediment can be characterized by a single grain size and use the *Meyer-Peter and Müller* [1948] formula to predict the bed load transport rate. This relation takes the form

$$q_{acd} = 8\left(\theta - \theta_c\right)^{3/2}\sqrt{R_s g d_{sd}^3} \tag{38}$$

where θ denotes the dimensionless Shields number, defined here as $\theta = C_f u_d^2/(R_s g d_{sd})$, and θ_c denotes the critical value of θ for incipient motion of sediment. In the above equation R_s is the submerged specific gravity

of sediment (= 1.65 for quartz), and d_{sd} is the characteristic sediment diameter. The parameters q_{ac} and $q_{ac,u}$, i.e., the derivative of q_{ac} with respect to u, can now be written in the dimensionless forms

$$q_{ac} = \left(\frac{u^2 - u_c^2}{1 - u_c^2} \right)^{3/2}, \tag{39a}$$

$$q_{ac,u} = \frac{3u \left(u^2 - u_c^2 \right)^{1/2}}{\left(1 - u_c^2 \right)^{3/2}} \tag{39b}$$

where u_c is the critical velocity for incipient sediment motion nondimensionalized by u_{td} and is defined in terms of a nondimensional critical bed shear stress θ_c, and the nondimensional bed shear stress θ_t corresponding to u_{td}. The parameters u_c and θ_t can be rewritten in the forms

$$u_c = \sqrt{\frac{\theta_c}{\theta_t}}, \tag{40a}$$

$$\theta_t = \frac{C_f u_{td}^2}{R_s g d_{sd}} \tag{40b}$$

In the succeeding section, we obtain u and η by solving (32) numerically.

3.7. Regularity Condition

As described above, the flow is in the Froude-subcritical regime in the upstream portion of a step, and in the Froude-supercritical regime in the downstream portion. Therefore, there must exist a point of transition from subcritical to supercritical regime somewhere on the step. The mathematical implication of this transition is that the denominator of the differential equation (32) changes sign from negative to positive and vanishes right at the transition. Let us denote the velocity at this transition as u_1. In the case of a nonerosional fixed bed, or an erosional bed composed of cohesive soil as analyzed by *Parker and Izumi* [2000], u_1 is equal to $Fr_t^{-2/3}$ in the present nondimensionalization. In the case of bedrock erosion considered in this paper, however, there is an extra term in the denominator of (32) associated with alluvial processes. As a result, u_1 is slightly larger than $Fr_t^{-2/3}$. Therefore, (32) would appear to have a singularity when $u = u_1$. No physically realistic solution for step shape can be obtained, however, were this singularity to prevail. In order to avoid it, the numerator must vanish as well. Thus, the following condition is required:

$$c = \frac{1 - q_{ac}^{-1}(u_1) - w_a}{u_1^3} \tag{41}$$

This is referred to as the regularity condition in this analysis.

As long as L_{mr} is small, and Fr_t is not close to unity, the deviation of u_1 from $Fr_t^{-2/3}$ is slight, but otherwise the term arising from the alluvial process has a significant effect on the analysis. In the case of the purely erosional process of cohesive soil [*Parker and Izumi*, 2000], $u_1 (= Fr_t^{-2/3})$ is always smaller than $u_L = u|_{x=L} (= 2/[\sqrt{1 + 8Fr_t^2} - 1])$ in the domain $0 \le Fr_t < 1$. In the case of bedrock erosion, however, u_1 may be larger than u_L when Fr_t is close to unity. When $u_1 > u_L$, the velocity at the transition u_1 is nowhere realized on a step. Thus, no regularity condition need be satisfied. But the consequence of this is that one relation among those needed to set the parameters c, w_a, and Fr_t is lost. In such a case, cyclic steps cannot be uniquely determined, and therefore, regular cyclic steps cannot be delineated from the assumptions made in this model. The condition for cyclic steps to be uniquely determined is $u_1 < u_L$, or correspondingly

$$Fr_t^2 u_L - u_L^{-2} - L_{mr} q_{ac,u}(u_L) q_{ac}^{-2}(u_L) > 0 \tag{42}$$

In Figure 6, the upper limit of Fr_t for the existence of steps is shown on the u_c-Fr_t plane. The solid, dashed, and dotted curves correspond to the cases $L_{mr} = 0.05$, 0.1, and 0.2, respectively. In the region above each curve, cyclic steps cannot be uniquely specified. It is found that the upper limit of Fr_t approaches unity as u_c approaches unity as well and takes a nearly constant value when u_c is sufficiently below unity. In addition,

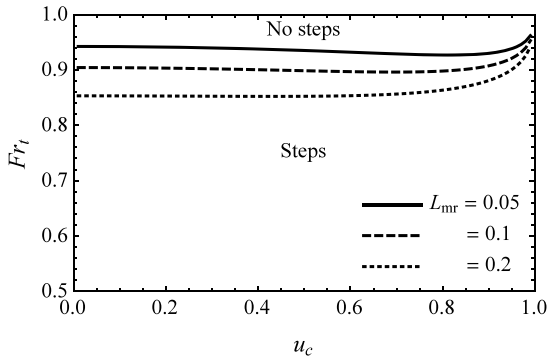

Figure 6. Upper limit of Fr_t as a function of u_c and L_{mr}.

the upper limit of Fr_t decreases with increasing L_{mr}. The sediment transport rate becomes large, and thus, the effect of alluvial processes in (42) (i.e., the effect of terms containing the parameter q_{ac}) becomes significant when Fr_t and L_{mr} are large, and u_c is sufficiently below unity. Therefore, the physical implication of Figure 6 is that cyclic steps cannot form when the effect of alluvial process becomes so significant that (42) cannot be satisfied. It should be recalled in this regard that no bedrock-alluvial cyclic steps can form over a completely alluviated bed, as illustrated in Figure 3a.

3.8. Upper and Lower Limits of w_a

We now consider the character of the boundary value problem associated with the first-order ordinary differential equation (32). For each set of specified values of the sediment supply rate per unit width q_{asd}, the water discharge per unit width q_{wd}, the average slope S, the bed friction coefficient C_f, and the two Froude numbers Fr_t and Fr_n are specified as well. Once the two Froude numbers are specified, the first-order differential equation (32) for $u(x)$ with the three unknown parameters c, w_a, and L can now be solved under the two boundary conditions (33) and (34), and the two additional constraints (37) and (41). The numerical solution of differential equation (32) for a set of specified values of two Froude numbers requires an iterative process. It is convenient to specify Fr_t and w_a and then compute Fr_n and the remaining parameters. In the numerical solution, w_a cannot be selected arbitrarily. There is an upper bound w_{au} and also a lower bound w_{al}, outside of which a solution cannot be realized. These bounds are specified below.

At the transition point from the subcritical to supercritical regime, (32) in conjunction with (41) takes an indeterminate form $\mathrm{d}u/\mathrm{d}x = 0/0$. Applying L'Hopital's rule, we obtain

$$\left.\frac{\mathrm{d}u}{\mathrm{d}x}\right|_{u=u_1} = \frac{u_1^3 q_{ac,u}(u_1) q_{ac}^{-2}(u_1)}{\left(1 - q_{ac}^{-1}(u_1) - w_a\right) Q} - \frac{3u_1^2}{Q} \tag{43}$$

$$Q = Fr_t^2 + 2u_1^3 + L_{mr} q_{ac}^{-2}(u_1) \left(2q_{ac,u}^2(u_1) q_{ac}^{-1}(u_1) - q_{ac,uu}(u_1)\right) \tag{44}$$

In (44), the term containing L_{mr} is generally small compared with $Fr_t^2 + 2u_1^3$, and, therefore, Q is found to take a positive value. Therefore, $\mathrm{d}u/\mathrm{d}x|_{u_1}$ becomes infinite as w_a approaches $1 - q_{ac}^{-1}(u_1)$ from below. When w_a is slightly larger than $1 - q_{ac}^{-1}(u_1)$, $\mathrm{d}u/\mathrm{d}x|_{u_1}$ takes a large negative value, which is not physically realistic because this means that the flow decelerates at the transition from the subcritical to supercritical regime. Thus, the following upper bound holds:

$$w_{au} = 1 - q_{ac}^{-1}(u_1) \tag{45}$$

The above equation in conjunction with (41) also implies that c must be positive, so that in accordance with the coordinate system defined above, cyclic steps always migrate in the upstream direction according to the present model.

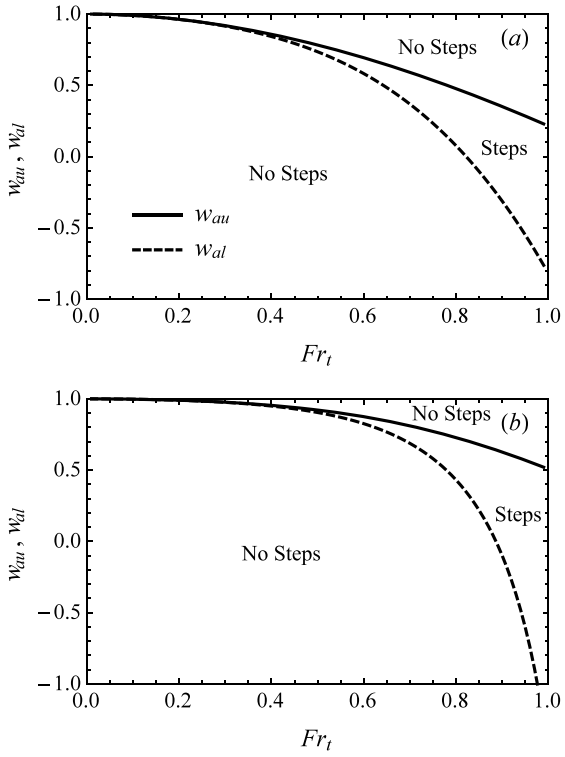

Figure 7. Lower and upper limits w_{au} and w_{al} on w_a as functions of Fr_t for the cases (a) $L_{mr} = 0.1$, $u_t = 0.2$, and (b) $L_{mr} = 0.1$, $u_t = 0.8$. The solid and dashed lines correspond to w_{au} and w_{al}, respectively.

The lower bound w_{al} is derived from the condition that the flow must accelerate over the whole domain of a step. As w_a decreases, the condition $du/dx < 0$ is first satisfied at the downstream end of the domain. Therefore, we require that $du/dx|_{u_L} > 0$. This condition may be rewritten in the form

$$\frac{\frac{1-q_{ac}^{-1}(u_L)-w_a}{1-q_{ac}^{-1}(u_1)-w_a}u_1^3 - u_L^3}{Fr_t^2 u_L - u_L^{-2} - L_{mr} q_{au,u}(u_L) q_{ac}^{-2}(u_L)} > 0 \tag{46}$$

Thus, the lower bound satisfying the above equation w_{al} is

$$w_{al} = 1 + \frac{u_1^3/q_{ac}(u_L) - u_L^3/q_{ac}(u_1)}{u_L^3 - u_1^3} \tag{47}$$

Figures 7a and 7b show w_{au} and w_{al} as functions of Fr_t for the cases $(L_{mr}, u_c) = (0.1, 0.2)$ and $(0.1, 0.8)$, respectively. In both figures, the solid and dashed curves indicate w_{au} and w_{al}, respectively. Cyclic steps of permanent form are possible only between the solid and dashed curves. In both cases, cyclic steps of permanent form can exist only within an ever-narrower range of values w_a close to unity when Fr_t becomes smaller than 0.5.

3.9. Solution Domains on the Fr_t-Fr_n Plane

The solution domain on the Fr_t-Fr_n plane for cyclic steps for the case $L_{mr} = 0.1$ and $u_c = 0.5$ is illustrated in Figure 8. It can be seen from Figure 8 that a necessary but insufficient condition for step formation is $Fr_t < 1$ and $Fr_n > 1$. The figure is obtained by calculating values of Fr_n as w_a is changed from w_{al} to w_{au} for a given value of Fr_t. The region in which cyclic steps are not solvable due to the lack of a regularity condition shown in Figure 6 is also shown on the right-hand side of Figure 8, i.e., in the range where Fr_t becomes greater than a value that is somewhat smaller than unity. While this upper limit on Fr_t changes somewhat with changing values of L_{mr} and u_c, the boundary between steps and no steps on the left-hand side of the figure depends only slightly on the values of L_{mr} and u_c.

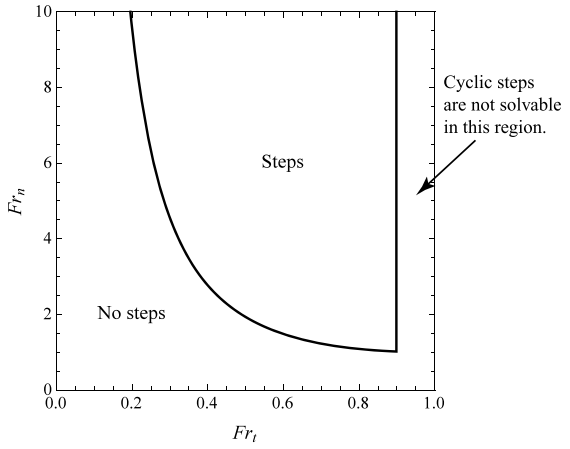

Figure 8. Solution domains on the Fr_t-Fr_n plane for cyclic steps for the case for which $L_{mr} = 0.1$ and $u_c = 0.5$.

According to Figure 8, near the upper limit $Fr_t = 0.9$, cyclic steps can exist over a wide range of Fr_n larger than unity. The solution domain is confined to the range of larger values of Fr_n as Fr_t decreases, however. It is found from (9a) and (9b) that u_{td} decreases, and thus, the sediment transport rate q_{asd} decreases with decreasing Fr_t. In addition, large values of Fr_n correspond to large values of the bed slope S according to (21a) and (21b). It follows that as the sediment transport rate becomes ever smaller, cyclic steps can be formed only in ever steeper channels.

As seen in Figure 10 and as is subsequently shown in this paper, when Fr_t is small, the cover fraction p is almost zero everywhere except in the vicinity of the upstream end of each step. Although a small value of p implies a small amount of sediment transport that may be insufficient to erode bedrock, steep bed slopes can enhance erosional efficiency. Therefore, a large bed slope may be required.

Parker and Izumi [2000] have expressed the nondimensional erosion rate of a bed composed of cohesive soil in the following form:

$$E = (u^2 - 1)^{\alpha} \tag{48}$$

They found that if α is larger than 1.5, cyclic steps can be formed over the whole domain of values of $Fr_t \in (0, 1)$ and $Fr_t < Fr_n$. On the other hand, if α is smaller than 1.5, cyclic steps can be formed only in a more restricted range of Fr_n. In the case of bedrock incision studied in this analysis, if the alluvial layer is ignored, the nondimensional incision function reduces to

$$E = 1 - q_{ac}^{-1}(u) = 1 - \left(\frac{1 - u_c^2}{u^2 - u_c^2}\right)^{3/2} \tag{49}$$

In the above equation, E asymptotically approaches unity as u increases. The behavior of the incision function (49) in the range of large u is similar to that of (48) with under the condition of relatively small α, so that cyclic steps can exist only within a restricted range of Fr_n in the case of bedrock incision.

4. Results and Discussion

4.1. Parameters and Step Profiles as Functions of Fr_n, Fr_t, and w_a

In Figures 9a–9c, the wavelength L, horizontal migration speed c, step height $\Delta\eta$, vertical additional degradation rate w_a, and cover fraction averaged over one wavelength $\bar{p}(= \bar{q}_{ac}^{-1})$ are plotted against Fr_n, for the respective values of Fr_t of 0.2, 0.4, and 0.6, and assuming $L_{mr} = 0.1$ and $u_c = 0.5$. It is found that in all these cases, L, c, and $\Delta\eta$ increase rapidly to approach ∞ as w_a approaches its lower bound w_{al}. Meanwhile, w_a and $\bar{p}$ increase to approach almost constant values in the range of sufficiently large Fr_n.

In accordance with Figure 8, when Fr_t is small, cyclic steps can exist only in the range of large values of Fr_n. In the case $Fr_t = 0.2$ in particular, cyclic steps cannot form if Fr_n is smaller than about 10. It is also found that the possible range of values of L, c, and $\bar{p}$ increase with increasing Fr_t.

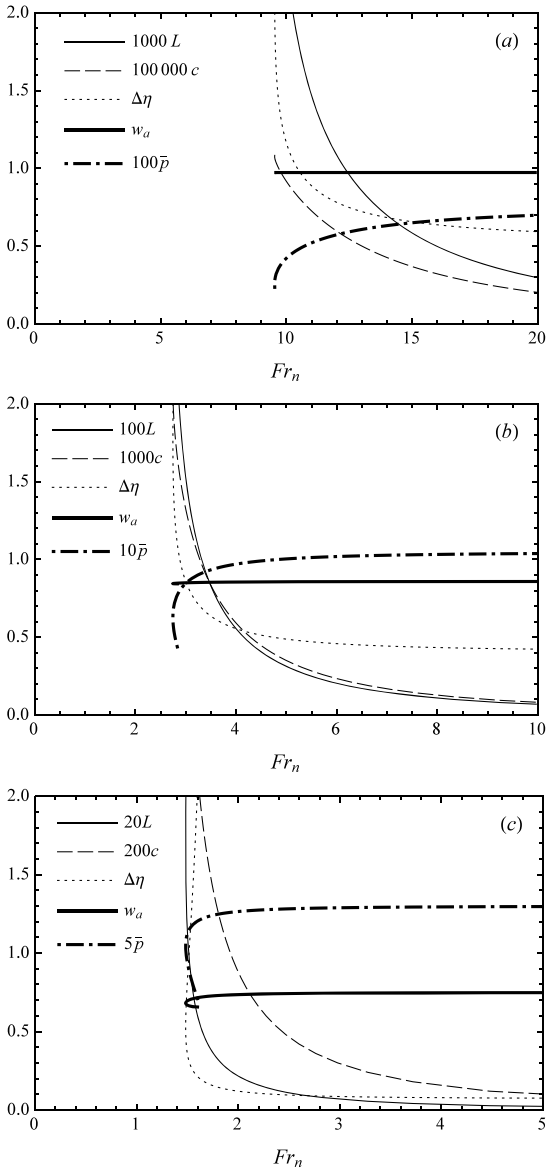

Figure 9. Parameters for cyclic steps as functions of Fr_n for the cases (a) $Fr_t = 0.2$, (b) $Fr_t = 0.4$, and (c) $Fr_t = 0.6$; $L_{mr} = 0.1$, $u_c = 0.5$. Note that while values of the vertical axis are constant, the variables are multiplied by different coefficients in the three plots in order to show all the variables in one figure.

As seen in Figure 7, the possible range of values of w_a becomes ever narrower when Fr_t becomes smaller than 0.5. Accordingly, in Figures 9a and 9b corresponding to the cases $Fr_t = 0.2$ and 0.5, respectively, w_a barely changes as Fr_n varies. In Figure 9c corresponding to the case $Fr_t = 0.6$, w_a is nearly constant in Fr_n, varying only slightly in the vicinity of the lower limit of Fr_n. In addition, in the range of Fr_n close to its lower limit, w_a can take two different values for a specified value of Fr_n. Consequently, the other corresponding parameters also become double valued near the lower limit of Fr_n. This implies that within a narrow range of values of Fr_n, two different states of cyclic steps are possible for a pair of specified values of Fr_t and Fr_n.

Although the issue of double-valued behavior is a minor one due the restricted conditions under which it occurs, it merits some explanation. The step height $\Delta\eta$ and wavelength L are both single-valued functions that increase monotonically with decreasing w_a. In the range of relatively large values of w_a, L increases faster than $\Delta\eta$, so that the slope S decreases monotonically with decreasing w_a. However, in the vicinity of the lower limit of w_a, there appears a region where the increase in $\Delta\eta$ overcomes the increase in L. In this region,

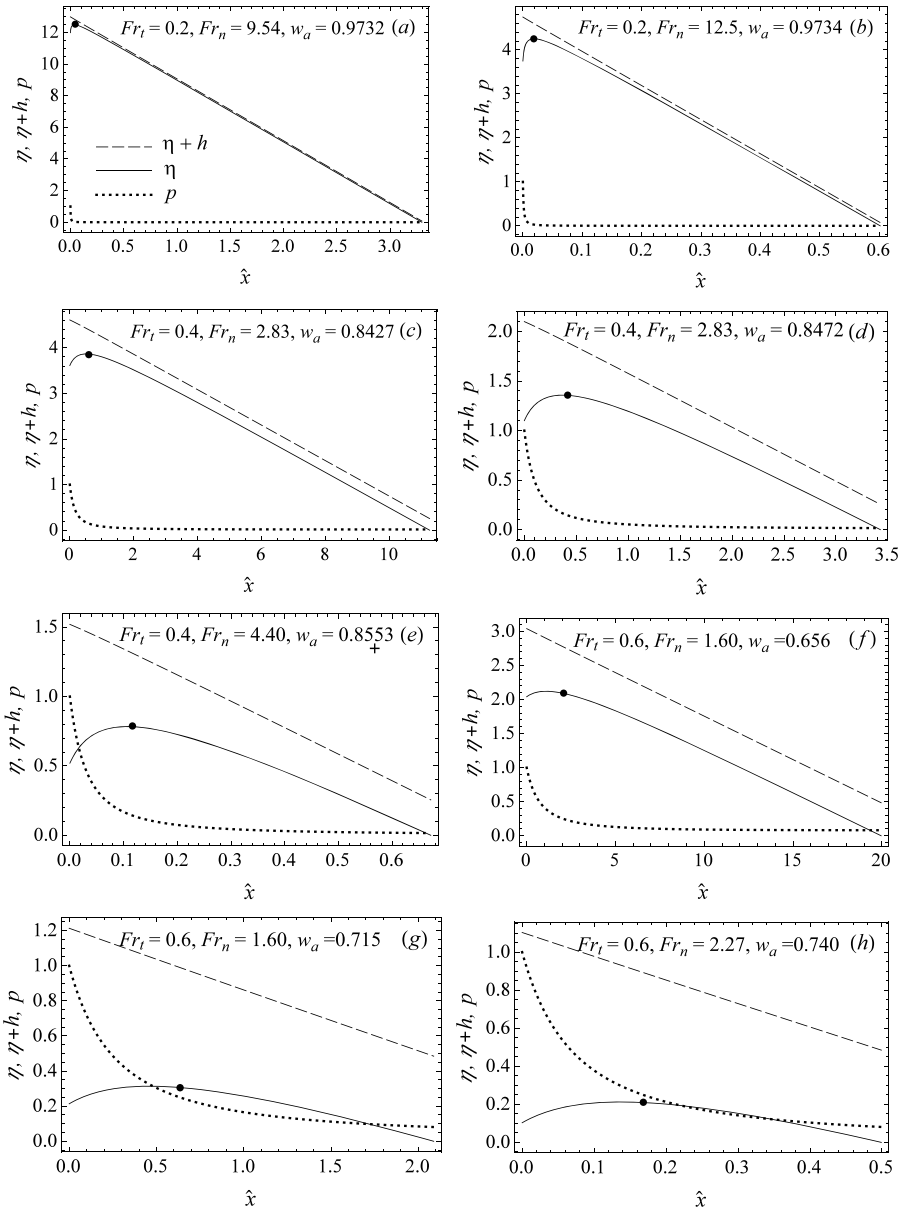

Figure 10. Profiles of the bed elevation η, the water surface elevation $\eta + h$, and the cover fraction p over a single cyclic step for $L_{mr} = 0.1$, $u_c = 0.5$, and (a) $Fr_t = 0.2$, $Fr_n = 9.54$, $w_a = 0.9732$; (b) $Fr_t = 0.2$, $Fr_n = 12.5$, $w_a = 0.9734$; (c) $Fr_t = 0.4$, $Fr_n = 2.83$, $w_a = 0.8427$; (d) $Fr_t = 0.4$, $Fr_n = 2.83$, $w_a = 0.8472$; (e) $Fr_t = 0.4$, $Fr_n = 4.40$, $w_a = 0.8553$; (f) $Fr_t = 0.6$, $Fr_n = 1.60$, $w_a = 0.656$; (g) $Fr_t = 0.6$, $Fr_n = 1.60$, $w_a = 0.715$; (h) $Fr_t = 0.6$, $Fr_n = 2.27$, $w_a = 0.740$. The solid, dashed and thick dotted lines indicate η, $\eta + h$, and p, respectively, and the dot denotes the point where the Froude-critical condition is achieved. Figures 10a and 10b show cases of relatively small sediment supply, and relatively mild and steep cases, respectively. Figures 10c–10e show cases of medium sediment supply; Figures 10c and 10d are cases of the same mean bed slope but different values of w_a, and Figure 10e is a case of a steeper slope. Figures 10f–10h are cases of large sediment supply; Figures 10f and 10g are cases of the same slope but different values of w_a, and Figure 10h is a case of a relatively steep slope. Note that the vertical scale varies between panels.

S consequently increases with decreasing w_a. In order to know which state of the two is actually realized, the stability of those two solutions should be studied. Further detailed analysis of this problem is left as a future problem.

In order to obtain a view of the variation of step shape as the two Froude numbers Fr_t and Fr_n are varied, a total of eight cases of profiles of bed elevation η, water surface elevation $\eta + h$, and cover fraction p over a single cyclic step are shown in Figures 10a–10h. The values $L_{mr} = 0.1$ and $u_c = 0.5$ have been used in the

computations. In the figures, the solid, dashed, and thick dotted curves illustrate η, $\eta + h$, and p, respectively. The dot on the bed denotes the point at which the Froude-critical condition is achieved. As described above, the vertical length scale for the nondimensionalization is smaller than the horizontal length scale by a factor of S_t. Correspondingly, the plots of η, $\eta + h$, and p against x have an inherent distortion. In order to remove the effect of this distortion from the plots, we renormalize the horizontal coordinate as follows:

$$\hat{x} = \frac{x}{S_t} = \frac{x_d}{h_{td}} \tag{50}$$

Assuming $C_f = 0.04$ in (9a) and (9b), the values of S_t are calculated to be 0.0016, 0.0064, and 0.0144 for the cases $Fr_t = 0.2$, 0.4, and 0.6, respectively. These values have been used in the computation of the parameter $\hat{x}$ in the plots.

Figures 10a and 10b correspond to the cases $(Fr_t, Fr_n, w_a) = (0.2, 9.54, 0.976)$, and $(0.2, 12.5, 0.973)$, respectively. It is seen from the figures that the bed slope is rather large when Fr_t is small and Fr_n is large, as discussed in regard to Figure 8. The present analysis uses forms of governing equations that apply only when the bed slope is not too high, i.e., when $\cos\phi \approx 1$ and $\sin\phi \approx \tan\phi = S$, with ϕ denoting the slope angle. At sufficiently steep slopes, even the longwave approximation breaks down. Results at very high slopes are nevertheless shown in order to illustrate the general characteristics of the solution. It is expected, however, that these results have some qualitative significance even outside the range of quantitative application.

Figures 10c–10e correspond to the cases $(Fr_t, Fr_n, w_a) = (0.4, 2.83, 0.843)$, $(0.4, 2.83, 0.8472)$, and $(0.4, 4.40, 0.855)$, respectively. In Figures 10c and 10d, two different forms of steps are obtained for the same value of $F_n = 2.83$ and the different values of w_a for $Fr_t = 0.4$. It can be seen that though the step in Figure 10c with a larger value of w_a has a longer wavelength than that in 10d with a smaller w_a, both have an identical average bed slope. An example with a larger value of Fr_n is shown in Figure 10e. It is found that as Fr_n increases, the average bed slope becomes too large for the present analysis to apply even if Fr_t is larger than 0.2.

In Figures 10f–10h, the profiles of η, $\eta + h$, and p are shown for the cases $(Fr_t, Fr_n, w_a) = (0.6, 1.60, 0.656)$, $(0.6, 1.60, 0.716)$, and $(0.6, 2.27, 0.740)$, respectively. The set of Figures 10f and 10g indicates that there exist two different forms of steps for the same value of $Fr_n = 1.6$ for $Fr_t = 0.6$. It is found that the wavelength and wave height of the step in Figure 10f are both approximately 10 times larger than those of the step in Figure 10g, so resulting in the same mean slope for both.

According to this analysis, then, the profile of a step is thus characterized by a relatively short, upstream subcritical portion which has an adverse bed slope in all the cases in Figure 10. According to *Parker and Izumi* [2000], in the case of purely erosional cohesive soil a local adverse slope can be preserved as long as w_a is positive at the upstream end of the step. In the present case of bedrock erosion, however, (31) does not immediately reduce to the same result as the purely erosional case; w_a must be positive at least for an adverse slope to be preserved at the upstream end. This is consistent with Figure 7, which shows that w_a takes a positive value over most of the range of Fr_t.

The shallow water formulation used in this analysis is insufficient to describe the formation of a plunge pool just downstream of the hydraulic jump. In reality, however, erosion may be activated by gravel deposited in the adversely sloping upstream portion, ultimately resulting in a fully excavated plunge pool. As seen in Figure 1b, cyclic steps observed in the field are often accompanied by plunge pools. The condition that the upstream portion of all the steps shown in Figure 10 have an adverse bed slope might be thought to abet the formation of a plunge pool. The morphodynamics of plunge pool excavation itself is a fascinating problem that is one step beyond the present analysis. Recent developments in this line of research can be found in *Scheingross et al.* [2015], *Scheingross and Lamb* [2016], and *Scheingross* [2016, chap. 6 therein].

Another important feature of step shape deserves emphasis. The downstream supercritical region is a relatively long and has a nearly constant bed gradient. As shown in (49), the nondimensional erosion function approaches a constant value of unity as u becomes sufficiently large. It is expected, therefore, that the erosion rate sufficiently far downstream, where the velocity becomes large, should approach a constant value. The slope profile of permanent form subject to uniform erosion can be nothing but a flat slope with a constant gradient. It follows that as long as (49) is used to describe the erosion process, a flat slope with a constant gradient can be expected to appear in the downstream portion of a step, as shown in Figure 10.

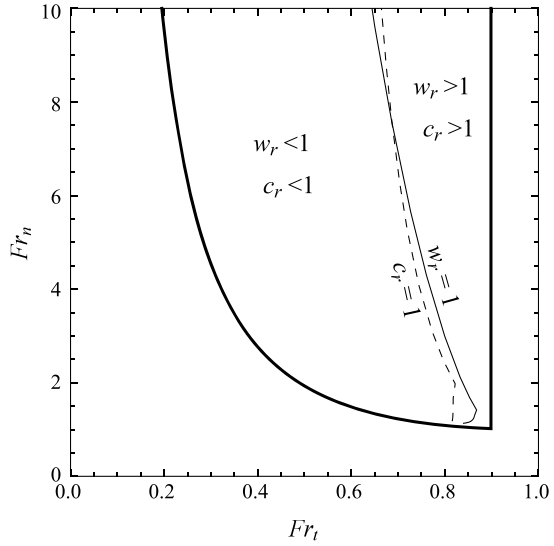

Figure 11. The boundary between the ranges where $w_r > 1$ and $w_r < 1$, and the boundary between the ranges where $c_r > 1$ and $c_r < 1$. $L_{mr} = 0.1$ and $u_c = 0.5$. The range $w_r > 1$ ($w_r < 1$) corresponds to an incision rate that is enhanced (suppressed) by the presence of steps, and the range $c_r > 1$ ($c_r < 1$) corresponds to an upstream migration rate that is enhanced (suppressed) by the presence of steps.

4.2. Effects of Steps on Bedrock Erosion

The question arises as to whether or not steps abet or inhibit incision, as compared to the case with no steps described in Figure 4. In order to study this issue, we define the following two ratios:

$$c_r = \frac{c}{c_n}, \quad w_r = \frac{w_s}{w_n} \tag{51}$$

That is, c_r and w_r denote the ratio of wave speed and total degradation rate, respectively, with and without steps. Once the two Froude numbers Fr_t and Fr_n are specified, c, w_s, c_n, and w_n are uniquely determined. Therefore, we can calculate the values of c_r and w_r in the Fr_t-Fr_n plane. Figure 11 is an extended version of Figure 8, in which zones where $c_r < 1$, $c_r > 1$, $w_r < 1$, and $w_r > 1$ are shown. It can be seen therein that for a given value of Fr_n, smaller values of Fr_t favor stepped beds that both incise and migrate upstream more slowly than the case of no steps, and larger values of Fr_t favor the opposite behavior. Of interest is the fact that the lines where $c_r = 1$ and $w_r = 1$ nearly coincide. This means that the upstream migration and the vertical incision are both amplified by the formation of steps in more or less the same region of the Fr_t-Fr_n plane, where Fr_t is large and therefore the sediment supply is large. In this region, bedrock erosion is generally activated by the formation of steps. On the other hand, if the sediment supply is relatively small, total bedrock erosion is reduced by the formation of cyclic steps in bedrock.

4.3. Cover Fraction p, Friction Coefficient C_f, and Direction of Incision

Several issues merit further discussion. In this paper, the cover fraction p and the ratio η_a/L_{mr} of alluvial thickness to macroroughness are related by (13). According to this relation, $p = 0$ when $\eta_a = 0$. *Zhang et al.* [2015] use a somewhat different relation, according to which p takes a small residual value when $\eta_a = 0$. The small residual value prevents the speed of an alluvial wave from taking an infinite value when $\eta_a = 0$. The physics corresponding to the need for this residual value are discussed in *Zhang et al.* [2015]; sediment particles can roll at high speed over a very smooth bed. It is not necessary to include this residual value in the present formulation, because the solution of permanent form is predicated on the condition that alluvial cover nowhere drops to zero.

Here it is assumed that the resistance coefficient C_f takes a prescribed value. Many authors, including *Nelson and Seminara* [2011], *Tanaka and Izumi* [2013], *Inoue et al.* [2015], and *Johnson* [2014] have suggested that C_f should be computed as a weighted average based on the resistance offered by alluvial particles in covered areas, and the resistance offered by bedrock macroroughness in exposed areas. The present analysis is easily extended to this case, which might yield interesting new results. But a first-order theory that captures the basic mechanisms of incisional steps of permanent form does not require this detail.

Similarly, the alluvial cover in typical bedrock rivers corresponds to a mixture of sizes. The present analysis could be extended to sediment mixtures using an appropriate sediment transport formulation, such as the *Ashida and Michiue* [1972] relation and an active layer formulation for the bed. We again point out, however, that a first-order theory of incisional cyclic steps does not require a consideration of mixtures. Having said this, a consideration of mixtures might result in noticeably different results for step morphology. If the volumetric transport capacity depends on the sediment size, the cover fraction p is a function of the sediment size as well. Therefore, the fraction of each sediment size range in the bed may depend on the location within a step. Because the ability to erode bedrock is determined by the sediment size, the erosion rate for a sediment mixture may differ from that for uniform sediment. This problem is worth consideration for the future.

We note that the present analysis is formally restricted to slopes that are not so steep that the $\cos\phi$ cannot be approximated as unity. In order to extend the analysis to such high slopes, not only do the shallow water equations need to be modified but also the direction of incision needs to be changed from (approximately) vertical downward to downward normal from the bed. Such changes, and also the changes necessary to capture plunge pool dynamics [e.g., *Scheingross and Lamb*, 2016], might best be implemented with a full numerical model.

4.4. Features of Cyclic Steps Predicted by the Model and Future Work for Validation

The results of our analysis warrant further investigation and validation through field observations and laboratory experiments. In particular, the following findings should be examined:

1. Our analysis predicts that incisional cyclic steps can form only within a specific range in the Fr_t-Fr_n plane. Therefore, if the data pertaining to Fr_t and Fr_n can be obtained for sites where incisional cyclic steps are observed, as well as sites where they are not observed, the solution domain predicted by the analysis can be validated.
2. According to our analysis, the wavelength L is determined by the values of Fr_t and Fr_n. Therefore, if data for L, Fr_t, and Fr_n can be obtained in the field or in experiments, the results of the analysis can be validated by comparing the observed wavelength L with the predicted one.
3. The bed profile over a single cyclic step predicted by the analysis is characterized by a relatively short upstream portion with an adverse gradient, and a long flat downstream portion with a constant slope. Although pertinent data are available for testing our predictions [e.g., *Yokokawa et al.*, 2015; *Scheingross et al.*, 2015; *Scheingross*, 2016, chap. 6 therein], the data are fairly limited, precluding confident evaluation at this time.

5. Conclusion

We propose a mathematical model to explain the formation of incisional cyclic steps in mixed bedrock-alluvial channels. The model is composed of the Macro-Roughness Saltation Abrasion Alluviation model for incisional and alluvial processes and the shallow water momentum and continuity equations. To perform the analysis, we employ several constraints, such as the cover factor being less than unity in the downstream steep portion of steps. These constraints are originally based on our conceptualization of the problem but are found to be consistent with field observations. The model is reduced to a first-order ordinary differential equation for the streamwise velocity profile and three unknown parameters. This equation is solved under two boundary conditions and two additional constraints. The analysis is greatly simplified with the use of the quasi-steady assumption for alluvial processes which we introduce here for the first time.

The salient results of our analysis are listed below.

1. Solutions for incisional cyclic steps of permanent form in mixed bedrock-alluvial rivers can be found within the range of Fr_t from 0 to 1 and Fr_n larger than 1. In the range of small Fr_t, such solutions exist only in the range of sufficiently large, Fr_n, while in the range of large Fr_t, they exist over a wide range of values of Fr_n larger than unity. The parameters Fr_t and Fr_n are related to the sediment supply and the average slope, respectively. Therefore, if the sediment supply is sufficiently small cyclic steps of permanent form can be expressed only on steep slopes. If the sediment transport rate is sufficiently large on the other hand, cyclic steps can be expressed on lower slopes. This is probably because, when the sediment supply is not sufficiently large, small amounts of sediment cannot effectively drive incision, so that large slopes are required to enhance the work done by the available sediment in forming cyclic steps.

2. Step shape is characterized by a relatively short upstream portion with an adverse gradient, and a long, rather flat downstream portion with a constant gradient. The former characteristic of the step shape is caused by the fact that the dimensionless vertical degradation rate additional to that caused by horizontal migration w_a is positive over most of the range of values of Fr_t. We suggest that an adverse gradient in a relatively short upstream portion might easily evolve into the plunge pool commonly observed at the downstream end of each cyclic step as illustrated in Figure 1b, and as observed experimentally by *Yokokawa et al.* [2013], *Scheingross et al.* [2015], and *Scheingross* [2016, chap. 6 therein]. The latter characteristic of the step shape is associated with the nondimensional erosion function (49). The erosion rate approaches a constant value of unity as the flow velocity becomes sufficiently large and is expected to be a constant value sufficiently far downstream as well. The slope profile of permanent form under a uniform erosion rate must thus be linear with a constant gradient.
3. The upstream migration and the vertical incision are both reduced by the formation of cyclic steps in the range of small Fr_t and increased in the range of large Fr_t. Larger values of Fr_t correspond to larger amounts of sediment supply. Therefore, the bedrock incision is intensified by the formation of cyclic steps when the amount of sediment supply is large, while it is reduced when the amount of sediment supply is small.

Notation

C_f bed friction coefficient.
c dimensionless horizontal migration rate of the bed profile.
c_d dimensional version of c.
c_n c at the equilibrium incision condition in the absence of steps.
c_{nd} dimensional version of c_n.
c_r ratio of horizontal migration rate with and without steps ($= c/c_n$).
d_{sd} characteristic sediment diameter.
E dimensionless erosion or incision rate.
E_d dimensional erosion or incision rate.
Fr Froude number.
Fr_n Fr at the equilibrium incision condition in the absence of steps.
Fr_t Fr at the incisional threshold state.
g gravitational acceleration ($= 9.8$ m/s^2).
h dimensionless flow depth.
h_d dimensional version of h.
h_t dimensionless flow depth at the incisional threshold state.
h_{td} dimensional version of h_t.
L dimensionless wavelength.
L_{mr} dimensionless macroroughness height.
L_{mrd} dimensional version of L_{mr}.
p areal fraction of the bed covered with alluvium.
p_n p at the equilibrium incision condition in the absence of steps.
Q derivative of the denominator of the right-hand side of (32) with respect to u evaluated at the Froude critical point ($u = u_1$).
q_a dimensionless net volumetric gravel transport per unit width.
q_{ad} dimensional version of q_{ad}.
q_{ac} dimensionless volumetric gravel transport capacity per unit width.
q_{acd} dimensional version of q_{ac}.
q_{acn} q_{ac} at the equilibrium incision condition in the absence of steps.
q_{acnd} dimensional version of q_{acn}.
q_{ad} dimensional net volumetric gravel transport rate per unit width.
q_{as} dimensionless sediment supply rate per unit width ($= 1$).
q_{asd} dimensional version of q_{as}.
q_{wd} dimensional flow discharge per unit width.
R_s submerged specific gravity of sediment ($= 1.65$).
S bed slope.
S_r bed slope relative to the threshold bed slope ($= S/S_t$).

S_t threshold bed slope.
t dimensionless time.
t_d dimensional version of t.
u dimensionless depth-averaged flow velocity.
u_1 dimensionless Froude critical velocity.
u_c dimensionless critical flow velocity for incipient sediment motion.
u_d dimensional version of u.
u_L u just upstream of a hydraulic jump.
u_n u at the equilibrium incision condition in the absence of steps.
u_{nd} dimensional version of u_n.
u_t dimensionless flow velocity at the incisional threshold state.
u_{td} dimensional version of u_t.
w_a dimensionless vertical degradation rate additional to that caused by horizontal migration.
w_{ad} dimensional version of w_a.
w_{al} lower bound of w_a.
w_{au} upper bound of w_a.
w_n dimensionless vertical degradation rate at the equilibrium incision condition in the absence of steps.
w_{nd} dimensional version of w_n.
w_r ratio of vertical degradation rate with and without steps ($= w_s/w_n$).
w_s dimensionless total vertical degradation rate in the presence of steps.
x dimensionless horizontal streamwise coordinate.
x_d dimensional version of x.
$\hat{x}$ x_d nondimensionalized by h_{td}.
$\tilde{x}$ dimensionless streamwise coordinate moving with steps.
α exponent of the erosion function of cohesive soil.
β abrasion coefficient.
γ ratio between the typical bed evolution rates due to bedrock incision and alluvial processes (incision-alluvial speed ratio).
$\Delta\eta$ dimensionless wave height (step height).
η dimensionless total bed elevation.
η_a dimensionless thickness of alluvium.
η_{ad} dimensional version of η_a.
η_b dimensionless elevation of bedrock.
η_{bd} dimensional version of η_b.
η_d dimensional version of η.
$\tilde{\eta}$ dimensionless bed elevation over steps of permanent form.
θ_t dimensionless bed shear stress correponding to u_{td}.
θ dimensionless bed shear stress ($\theta = C_f u_d^2/(R_s g d_{sd})$).
θ_c critical value of θ for incipient sediment motion.
λ porosity of alluvium.
ξ dummy integral variable.
ρ density of water ($= 1000$ kg/m^3).
ϕ bed slope angle.
τ_{bd} dimensional bed shear stress.
$\{\}_d$ dimensional variables.
$\{\}_{,u}$ partial derivative with respect to u.

Acknowledgments
The Mathematica program used in this paper is available at http://earth-fe.eng.hokudai.ac.jp/izumin/. This study was partially supported by the River Foundation in Japan. Part of this research was conducted during the third author's 3 months stay in Hokkaido University. The financial support for his stay from Hokkaido University is greatly appreciated. The authors express their gratitude to the Associate Editor and referees, whose careful review has greatly improved the paper.

References

Ashida, K., and M. Michiue (1972), Study on hydraulic resistance and bedload transport rate in alluvial streams [in Japanese], *Trans. Jpn. Soc. Civil Eng.*, *206*, 59–69.
Ashida, K., T. Takahashi, and T. Sawada (1981), Processes of sediment transport in mountain stream channels, in *Erosion and Sediment Transport in Pacific Rim Steeplands*, vol. 132, edited by T. R. H. Davies and A. J. Pearce, pp. 166–178, IAHS, Washington, D. C.
Balmforth, N., and A. Vakil (2012), Cyclic steps and roll waves in shallow water flow over an erodible bed, *J. Fluid Mech.*, *695*, 35–62.
Benda, L., and T. Dunne (1997a), Stochastic forcing of sediment supply to channel networks from landsliding and debris flow, *Water Resour. Res.*, *33*(12), 2849–2863.
Benda, L., and T. Dunne (1997b), Stochastic forcing of sediment routing and storage in channel networks, *Water Resour. Res.*, *33*(12), 2865–2880.

Duckson, D. W., and L. J. Duckson (1995), Morphology of bedrock step pool systems, *J. Am. Water Resour. Assoc.*, *31*, 43–51, doi:10.1111/j.1752-1688.1995.tb03362.x.
Fildani, A., W. R. Normark, S. Kostic, and G. Parker (2006), Channel formation by flow stripping: Large-scale scour features along the Monterey East Channel and their relation to sediment waves, *Sedimentology*, *53*(6), 1265–1287.
Goode, J. R., and E. Wohl (2010a), Substrate controls on the longitudianl profile of bedrock channels: Implications for reach-scale roughness, *J. Geophys. Res.*, *115*, F03018, doi:10.1029/2008JF001188.
Goode, J. R., and E. Wohl (2010b), Coarse sediment transport in a bedrock channel with complex bed topography, *Water Resour. Res.*, *46*, W11524, doi:10.1029/2009WR0008135.
Inoue, T., N. Izumi, M. onemoto, and K. Asahi (2011), Experimental study of erosion rate and critical tractive force on soft rock [in Japanese], *Adv. River Eng.*, *17*, 77–82.
Inoue, T., G. Parker, T. Iwasaki, Y. Shimizu, N. Izumi, C. Stark, and J. Funaki (2015), Numerical simulation of effects of sediment supply on bedrock channel morphology, *J. Hydraul. Eng.*, *142*(7), 4016014, doi:10.1061/(ASCE)HY.1943-7900.0001124.
Istanbulluoglu, E., D. G. Tarboton, R. T. Pack, and C. H. Luce (2004), Modeling of the interactions between forest vegetation, disturbances, and sediment yields, *J. Geophys. Res.*, *109*, F01009, doi:10.1029/2003JF000041.
Izumi, N., and M. Yokokawa (2011), *Cyclic Steps Formed in Bedrock Rivers*, IAHR, Beijing, China, 6–8 Sept.
Izumi, N., M. Yokokawa, and G. Parker (2012), Cyclic step morphology formed on bedrock [in Japanese], *J. Jpn. Soc. Civil Eng. Div. B*, *68*(4), I_955–I_960.
Johnson, J. P. L. (2014), A surface roughness model for predicting alluvial cover and bed load transport rate in bedrock channels, *J. Geophys. Res. Earth Surf.*, *119*, 2147–2173, doi:10.1002/2013JF003000.
Karlstrom, L., A. Zok, and M. Manga (2014), Near-surface permeability in a supraglacial drainage basin on the Llewellyn Glacier, Juneau Icefield, British Columbia, *Cryosphere*, *8*, 537–546, doi:10.5194/tc-8-537-2014.
Kostic, S., and G. Parker (2006), The response of turbidity currents to a canyon–fan transition: Internal hydraulic jumps and depositional signatures, *J. Hydraul. Res.*, *44*(5), 631–653.
Kostic, S., O. Sequeiros, B. Spinewine, and G. Parker (2010), Cyclic steps: A phenomenon of supercritical shallow flow from the high mountains to the bottom of the ocean, *J. Hydro-Environ. Res.*, *3*(4), 167–172.
Meyer-Peter, E., and R. Müller (1948), Formulas for bed-load transport, paper presented at 2nd Meeting, IAHR, Stockholm, Sweden.
Montgomery, D. M., and J. M. Buffington (1997), Channel-reach morphology in mountain drainage basins, *Geol. Soc. Am. Bull.*, *109*(5), 596–611.
Mori, R., T. Ishikawa, K. Osada, and S. Fukuoka (2010), Field experiments for recovery technique of riverbed level against bed degradation in the Asa River [in Japanese], *Adv. River Eng.*, *16*, 113–118.
Nelson, P. A., and G. Seminara (2011), Modeling the evolution of bedrock channel shape with erosion from saltating bed load, *Geophys. Res. Lett.*, *38*, L17406, doi:10.1029/2011GL048629.
Parker, G., and N. Izumi (2000), Purely erosional cyclic and solitary steps created by flow over a cohesive bed, *J. Fluid Mech.*, *419*, 203–238.
Reid, L. M. (1989), Channel incision by surface runoff in grassland catchments, PhD thesis, Univ. of Wash.
Scheingross, J. S., B. M. Fuller, and M. P. Lamb (2015), Autocyclic formation, retreat, and destruction of waterfalls in an experimental bedrock channel, paper presented at 2015 Fall Meeting, AGU, San Francisco, Calif., 14–18 Dec.
Scheingross, J. S., and M. P. Lamb (2016), Sediment transport through self-adjusting, bedrock-walled waterfall plunge pools, *J. Geophys. Res. Earth Surf.*, *121*, doi:10.1002/2015JF003620.
Scheingross, J. S. (2016), Mechanics of sediment transport and bed erosion in steep landscapes, PhD thesis, Calif. Inst. of Technol.
Sklar, L. S., and W. E. Dietrich (2004), A mechanistic model for river incision into bedrock by saltating bed load, *Water Resour. Res.*, *40*, W06301, doi:10.1029/2003WR002496.
Smith, I. B., J. W. Holt, A. Spiga, A. D. Howard, and G. Parker (2013), The spiral troughs of Mars as cyclic steps, *J. Geophys. Res. Planets*, *118*, 1835–1857, doi:10.1002/jgre.20142.
Sun, T., and G. Parker (2005), Transportational cyclic steps created by flow over an erodible bed. Part 2. Theory and numerical simulation, *J. Hydraul. Res.*, *43*(5), 502–514, doi:10.1080/00221680509500148.
Tadatsu, T., T. Suzuki, T. Uchida, and S. Fukuoka (2009), Secular variation of the elevation of exposed bedrock in the Tama River, paper presented at 64th Annual Meeting of JSCE, Fukuoka, Japan, 2–4 Sept.
Tanaka, G., and N. Izumi (2013), The bedload transport rate and hydraulic resistance in bedrock channels partly covered with gravel [in Japanese], *J. Jpn. Soc. Civil Eng. B*, *69*(4), I_1033–I_1038.
Tanise, A., Y. Watanabe, and Y. Yoshikawa (2008), *Cause of Rapid Degradation of a River Running Through a Volcanic Ash Zone*, Hokkaido Development Bureau, Sapporo, Japan, 20, 21 Feb.
Yamamoto, K. (2010), Effects of cohesive soil and soft rock on river channel characteristics, Tech. Rep., River Environ. Res. Inst., River Foundation, vol. 29, Tokyo, Japan.
Yokokawa, M., A. Kotera, A. Kyogoku, and N. Izumi (2013), *Cyclic Steps by Bedrock Incision, Advances in River Sediment Research*, edited by Fukuoka et al., Taylor and Francis, pp. 629–633, London, U. K.
Yokokawa, M., A. Kyogoku, and N. Izumi (2015), An experimental study for morphology of cyclic steps on model bedrocks [in Japanese], *J. Jpn. Soc. Civil Eng. B*, *71*(4), I_997–I_1002.
Yokokawa, M., N. Izumi, T. Naito, G. Parker, T. Yamada, and R. Greve (2016), Cyclic steps on ice, *J. Geophys. Res. Earth Surf.*, *121*, 1023–1048, doi:10.1002/2015JF003736.
Yonezawa, H., S. Fukuoka, and S. Suzuki (2007), Research on bed surface materials around a flow attack point and bed scouring [in Japanese], *Adv. River Eng.*, *13*, 345–350.
Zhang, L., G. Parker, C. P. Stark, T. Inoue, E. Viparelli, X. Fu, and N. Izumi (2015), Macro-roughness model of bedrock-alluvial river morphodynamics, *Earth Surf. Dynam.*, *3*, 113–138, doi:10.5194/esurf-3-113-2015.